Search for narrow nucleon resonances below pion threshold in the H(e,e′π+)X and 2H(e,e′p)X reactions

Kohl, M.; Ases Antelo, M.; Ayerbe, C.; Baumann, D.; Bohm, R.; Bosnar, Damir; Ding, M.; Distler, M. O.; Friedrich, J.; Garcia Llongo, J.; ...

Source / Izvornik: **Physical Review C - Nuclear Physics, 2003, 67**

Journal article, Published version
Rad u časopisu, Objavljena verzija rada (izdavačev PDF)

https://doi.org/10.1103/PhysRevC.67.065204

Permanent link / Trajna poveznica: https://urn.nsk.hr/urn:nbn:hr:217:769911

Search for narrow nucleon resonances below pion threshold in the $H(e,e'\pi^+)X$ and $^2H(e,e'p)X$ reactions

M. Kohl,[1,*] M. Ases Antelo,[2] C. Ayerbe,[2] D. Baumann,[2] R. Böhm,[2] D. Bosnar,[3] M. Ding,[2] M. O. Distler,[2] J. Friedrich,[2] J. García Llongo,[2] P. Jennewein,[2] G. Jover Mañas,[2] H. Merkel,[2] P. Merle,[2] U. Müller,[2] R. Neuhausen,[2] L. Nungesser,[2] R. Pérez Benito,[2] J. Pochodzalla,[2] M. Potokar,[4] C. Rangacharyulu,[5] A. Richter,[1,†] G. Schrieder,[1] M. Seimetz,[2] Th. Walcher,[2] and M. Weis[2]

[1]*Institut für Kernphysik, Technische Universität Darmstadt, D-64289 Darmstadt, Germany*
[2]*Institut für Kernphysik, Universität Mainz, D-55099 Mainz, Germany*
[3]*Department of Physics, University of Zagreb, HR-10002 Zagreb, Croatia*
[4]*Institute "Jožef Stefan," University of Ljubljana, SI-1001 Ljubljana, Slovenia*
[5]*Department of Physics, University of Saskatchewan, Saskatoon, Saskatchewan, Canada S7N 5E2*

(Received 18 December 2002; published 25 June 2003)

In two series of high-resolution coincidence experiments at the three-spectrometer facility at MAMI, the $H(e,e'\pi^+)X$ and $^2H(e,e'p)X$ reactions were studied to search for narrow nucleon resonances below pion threshold. The missing-mass resolution was 0.6–1.6 MeV/c^2 full width at half maximum in the proton experiment and 0.9–1.3 MeV/c^2 in the deuteron experiment. The experiments covered the missing-mass region from the neutron mass up to about 1050 and 1100 MeV/c^2, respectively. None of our measurements showed a signal for narrow resonances to a level of down to 10^{-4} with respect to the neutron peak in the missing-mass spectra.

DOI: 10.1103/PhysRevC.67.065204 PACS number(s): 14.20.Gk, 12.38.Qk

I. INTRODUCTION

It is an important issue of modern experiments in hadron physics to provide significant information on the manifestations of QCD. As is well known (see, e.g., Ref. [1]), the description of the experimentally observed baryon excitation spectrum in terms of the colorless three-quark (q^3) configuration within the various quark models has been quite successful. Moreover, QCD allows for exotic structures such as multiquark configurations, glueballs, and hybrids. Such states are mainly expected in the mass region above 1.5 GeV/c^2. It is one of the irritating facts, however, that already the q^3 description predicts far more resonance states than experimentally observed. Thus, the search for missing resonances is one of the major concerns of hadron experiments. On the other hand, the existing low-lying states (nucleon, Δ, N^*) are well accounted for within the three-quark picture and neither QCD-inspired calculations at low momentum and close to the chiral limit (i.e., chiral perturbation theory) nor perturbative QCD in the high-momentum regime predict states below or close to pion threshold. If such low-lying states did exist, configurations beyond the naive q^3 picture would be required for an explanation.

Since the strong decay via pion emission is energetically forbidden for states below pion threshold, these states would necessarily be narrow (less than a few keV) with lifetimes typical of electromagnetic or weak decays. A precise examination of the low-lying nucleon excitation spectrum with various probes is thus a powerful tool to test QCD.

Recently, there have been two experiments reported in the literature, one performed at the SATURNE synchrotron in Saclay and the other at the INR in Moscow, which claimed the observation of excited states of the nucleon below pion threshold [2,3]. Tatischeff *et al.* utilized the $H(p,p'\pi^+)X$ reaction to measure the invariant-mass spectrum of the missing nucleon [2]. They claimed to have found resonance states at $M_X = 1004$, 1044, and 1094 MeV/c^2, with a statistical significance of up to 17 standard deviations. However, the missing-mass resolution of this experiment was limited and ranged from 7 to 25 MeV/c^2 [full width at half maximum, (FWHM)]. Very recently, Tatischeff *et al.* reported further the observation of additional states at 1136, 1173, 1249, 1277, 1384, and possibly 1339 MeV/c^2 using the $H(p,p'\pi^+)X$, $^2H(p,p'p)X$, and $H(p,p'p)$ reactions [4].

Fil'kov *et al.* [3] found resonance structures in the $^2H(p,p'p)X$ reaction in the spectra of the invariant masses M_{pX} as well as M_X and claimed the observation of "supernarrow" dibaryons (SND) at $M_{pX} = 1904$, 1926, and 1942 MeV/c^2. The additionally observed resonance structures at $M_X = 966$, 986, and 1003 MeV/c^2 differ from those reported in M_{pX} by about one nucleon mass. They were interpreted to be either genuine, i.e., SND $\rightarrow p+X$, or to result from the decay SND $\rightarrow p+n+\gamma$ under the restrictions of a small phase space and experimental acceptance. The significance for the SND peaks was estimated to be 6 to 7 standard deviations, with a moderate missing-mass resolution of about 5 MeV/c^2.

So far, various attempts for an explanation of the narrow resonances [2,3] have been offered. Model assumptions beyond the q^3 picture result in mass formula prescriptions based on colored [5] and colorless [6] quark clusters. It has been argued [7], however, that narrow nucleon resonances should be completely excluded, since they were not observed in real Compton scattering experiments [8]. Another ap-

*Present address: MIT-Bates Linear Accelerator, Middleton, MA 01949.
†Corresponding author. Email address: richter@ikp.tu-darmstadt.de

proach describes the narrow resonances as possible members of the SU(6) spin-flavor multiplet, where only the two-photon transition channel is allowed [9]. This picture accounts for the fact that narrow resonances were not observed in photon-induced reactions like in real Compton scattering experiments. Recently, it was proposed to interpret the narrow states as collective excitations of the quark condensate through the multiple production of ''genuine'' Goldstone pions with a light mass of $m \approx 20$ MeV/c^2 [10]. In this model, the narrow states are spatially extended structures and thus they are likely inaccessible to the real photon probe.

Another theoretical interest in the narrow baryons is their influence on astrophysical objects. It was pointed out that the existence of narrow nucleon resonances would drastically affect the structure of neutron stars by lowering their possible maximal mass, which would be inconsistent with the observations [11]. However, the existence of light pions would still be compatible with the observed masses of neutron stars.

Meanwhile, there have been reported experiments in direct response to Tatischeff's and Fil'kov's findings. In a pilot study of the $\mathrm{H}(e,e'\pi^+)X$ reaction at the Jefferson Laboratory [12], the yield ratio $\mathrm{H}(e,e'\pi^+)X/\mathrm{H}(e,e'\pi^+)n$ was measured, which excludes narrow nucleon resonances to a level of 10^{-3}. The $^2\mathrm{H}(p,p'p)X$ reaction has been revisited at the RCNP in Osaka [13], yielding a null result for the above claimed states. However, the significance of the result of the latter experiment has been questioned in Ref. [14]. In fact, we have also reanalyzed the data of the virtual Compton scattering experiments at MAMI, but we did not find any signal above a significance of three standard deviations. In a photoproduction experiment at MAMI, the reactions $\mathrm{H}(\gamma,\pi^+\gamma n)$ and $\mathrm{H}(\gamma,\pi^+\gamma\gamma n)$ have been measured with a high luminosity and results are awaited [15].

The issue of the occurrence of resonances below pion threshold is thus unsettled. The observation of such narrow states is always limited by the achievable resolution. Experiments providing highest resolution are therefore best suited to perform such studies. In this paper, we report the results of two series of high-resolution measurements using the $\mathrm{H}(e,e'\pi^+)X$ and $^2\mathrm{H}(e,e'p)X$ reactions. The first reaction has been chosen as the analogous reaction to the $\mathrm{H}(p,p'\pi^+)X$ process of Tatischeff *et al.* [2]. The energy transfer corresponds to the excitation region of the Δ resonance. With the detection of the scattered electron in coincidence with the produced pion the missing mass of the reaction has been reconstructed. The experiment covered the missing-mass region from the neutron mass up to about 1050 MeV/c^2. In addition, the second electromagnetic reaction $^2\mathrm{H}(e,e'p)X$ has been studied as the analog of the strong $^2\mathrm{H}(p,p'p)X$ experiment by Fil'kov *et al.* [3]. The energy transfer varied from close to the threshold of the deuteron breakup up to the quasielastic region. With the detection of both the scattered electron and the emitted proton, the missing mass of the reaction has been reconstructed. The experiment covered the missing-mass region from the neutron mass up to about 1100 MeV/c^2.

II. MEASUREMENTS

The measurements were carried out at the three-spectrometer facility of the A1 Collaboration at the Mainz Microtron MAMI [16]. The target was a standard liquid hydrogen/deuterium target, which was operated at beam currents of up to 15 μA. The target cell has been made of a thin HAVAR foil of 10.2-μm thickness (8.9 μm in case of the deuterium target). The cell geometry is stadionlike with a length of 5 cm along the beam axis and a width of 1 cm in the perpendicular direction. The beam was swept before entering the scattering chamber to fill a square of 4×4 mm^2 on the target. The three magnetic spectrometers *A*, *B*, and *C* have been used for the detection of the scattered electrons and of the pions or protons of the respective reactions. The spectrometers are equipped with vertical drift chambers for tracking, a thin and a thick layer of plastic scintillators for the trigger and for π^+/p discrimination, and a large-volume gas Čerenkov counter for $e^\pm/\pi^\pm$ identification. The setup allows for very clean and high-resolution ($\Delta p/p \lesssim 10^{-4}$, $\Delta\theta \lesssim 3$ mrad) coincidence measurements yielding missing-mass resolutions of typically 1 MeV/c^2 (FWHM).

A. The $\mathrm{H}(e,e'\pi^+)X$ reaction

The first pilot measurement in the $\mathrm{H}(e,e'\pi^+)X$ reaction based on our proposal to the Program Advisory Committee at MAMI [17] was carried out in July 2000 with a total runtime of 18 h. The missing-mass spectrum showed a resonancelike structure around $M_X \approx 1007$ MeV/c^2, with a width of about 1 MeV/c^2, i.e., with the resolution of the setup. However, the significance was only ≈ 3 standard deviations, not warranting an interpretation of this finding as a positive identification.

A dedicated $\mathrm{H}(e,e'\pi^+)X$ experiment was thus performed in February and August 2002 with a total runtime of 257 h. The parameters of the kinematical settings are listed in Table I.

The scattered electrons were detected in spectrometer *B* at forward angles, and both spectrometer *A* and *C* were used in coincidence with *B* to detect the pions along the momentum-transfer direction (pion center-of-mass angle $\theta_\pi^* \approx 0°$), and almost perpendicular to it ($\theta_\pi^* \approx 100°$ and 110°), respectively. Most of the *AB* and *BC* measurements were carried out simultaneously, exploiting the full capabilities of the three-spectrometer facility.

The resolution of the measured coincidence time, after applying corrections due to individual path lengths and detector-related influences on the timing signals, varied from 0.8 to 1.2 ns (FWHM). The true events were selected by a ± 1.5-ns cut on the coincidence time spectrum. The shape of the background has been determined by selecting purely random coincidences. Furthermore, the data were normalized to the collected charge and the target thickness and were corrected for deadtime effects. The loss of pions due to their decay in flight from the origin to the detector has been corrected by weighting each pionic event with an individual survival probability, depending on the pion momentum and on the length of the pion track. The acceptance was determined by a simulation code, which accounts for the energy loss in the target and window materials of the scattering chamber and the spectrometer entrance, as well as for the Bethe-Heitler radiation of the electrons. After subtraction of

TABLE I. Kinematics of the H$(e,e'\pi^+)X$ reaction. The columns $p_{e'}$ ($\theta_{e'}$) and p_{π^+} (θ_{π^+}) are the central momenta and angles of the spectrometers. Also shown are the four-momentum transfer Q^2, the γ^*p invariant mass W, and the pion center-of-mass angle θ_π^*. The average beam current I and the net runtime T are shown in the rightmost columns. The settings H-1, 2, and 3 refer to the measurements with spectrometers A and B; settings H-4, 5, and 6 with B and C, respectively.

Kinematics	E_0 (MeV)	$\theta_{e'}$	θ_{π^+}	$p_{e'}$ (MeV/c)	p_{π^+} (MeV/c)	Q^2 (GeV^2/c^2)	W (MeV/c^2)	θ_π^*	I (μA)	T (h)
(AB)										
H-1	855.1	17.4°	22.4°	510	290	0.04	1220	0°	5.3	2.0
H-2	855.1	17.4°	22.4°	510	225	0.04	1220	0°	7.0	50.8
H-3	855.1	17.4°	22.4°	510	236	0.04	1220	0°	6.7	26.4
(BC)										
H-4	855.1	17.4°	55.0°	510	215	0.04	1220	100°	5.3	2.2
H-5	855.1	17.4°	55.0°	510	150	0.04	1220	100°	6.9	79.8
H-6	659.7	20.3°	88.4°	150	290	0.0125	1350	110°	14.3	96.0

the random background and application of the mentioned corrections, normalized yields for the H$(e,e'\pi^+)X$ reaction have been obtained.

Figures 1 and 2 summarize the results of the H$(e,e'\pi^+)X$ measurements. In the upper halves of Figs. 1 and 2, the normalized yields of three kinematical settings are presented as a function of the missing mass. The missing-mass resolution was $\approx$0.6 MeV/c^2 (FWHM) for the AB runs shown in Fig. 1, and $\approx$1.5–1.6 MeV/c^2 for the BC runs plotted in Fig. 2. The invariant masses of the states claimed by Tatischeff *et al.* [2] and Fil'kov *et al.* [3] are indicated by the vertical arrows. As is seen from the spectra, no significant narrow structure other than the peak corresponding to the ground state of the neutron is found. The missing-mass region from $M_X \approx 950$–1050 MeV/c^2 shows a smooth radiation tail. The measurements include a repetition of the kinematics of the pilot run (settings H-2/H-3 in Fig. 1) with about five times the statistics of the first run. In order to quantify the sensitivity of our measurements, we show yield ratios in the lower halves of Figs. 1 and 2. They are obtained by subtracting the radiation tail, modeled by a fifth-order polynomial, and dividing the spectra by the height of the respective neutron peak. The differential cross section for the H$(e,e'\pi^+)n$ channel can be estimated using the unitary isobar model "MAID" [18]. For the three kinematics of Figs. 1, 2(a), and 2(b), one obtains $d^3\sigma/(d\Omega_{e'}dE_{e'}d\Omega_\pi^*) \approx 2.6\times10^{-4}$, 8.2×10^{-4}, and 1.9×10^{-5} μb/(sr^2 MeV). As the yield ratios in the lower halves indicate, narrow structures can be excluded to a level of 10^{-4}, 10^{-3}, and 2×10^{-3} with respect to the

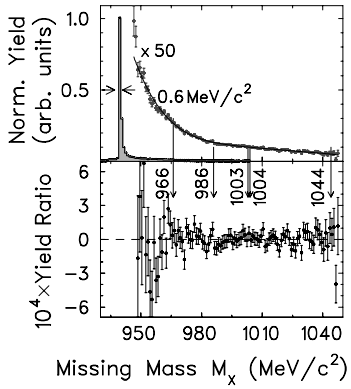

FIG. 1. Upper half: Missing-mass spectrum of the H$(e,e'\pi^+)X$ reaction, measured with spectrometers A and B at $\theta_\pi^*=0°$. The plot shows the result of setting H-1 (with the neutron peak height set to unity) and the combined settings H-2 and H-3 (at the electron beam energy and spectrometer settings listed in Table I). The achieved missing-mass resolution is 0.6 MeV/c^2 (FWHM) as given by the width of the neutron peak. A fifth-order polynomial is fit to the data to model the radiation tail. The invariant masses of the states claimed by Refs. [2,3] are indicated by the arrows. Lower half: Yield ratio of the above spectrum after subtraction of the radiation tail and division by the height of the neutron peak. Narrow structures (see the experiments of Refs. [2,3]) are excluded to a level of 10^{-4} of the height of the neutron peak.

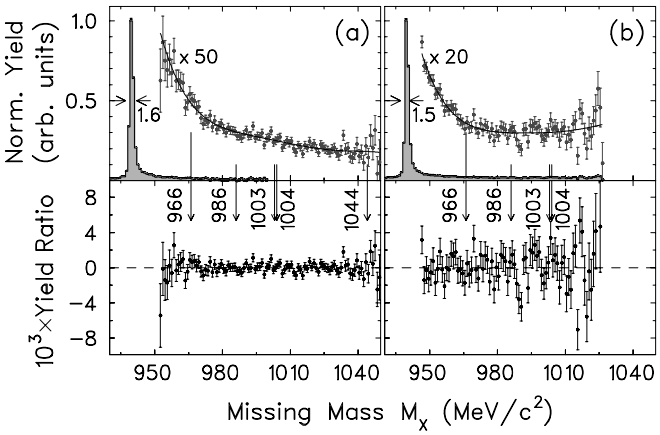

FIG. 2. Upper half: Missing-mass spectra of the H$(e,e'\pi^+)X$ reaction, measured with spectrometers B and C at $\theta_\pi^*\approx100°$. Plot (a) shows the settings H-4 (with the neutron peak height set to unity) and H-5, and (b) setting H-6 (at the electron beam energy and spectrometer settings listed in Table I). The achieved missing-mass resolution is (a) $\approx$1.6 MeV/c^2 (FWHM) and (b) $\approx$1.5 MeV/c^2, respectively. The vertical arrows are the same as in Fig. 1. The solid curves and the yield ratios in the lower half are obtained in the same way as in Fig. 1. Narrow structures (see the experiments of Refs. [2,3]) are excluded to a level of (a) 10^{-3} and (b) 2×10^{-3} of the height of the neutron peak, respectively.

TABLE II. Kinematics of the ^{2}H$(e,e'p)X$ reaction. The columns $p_{e'}$ ($\theta_{e'}$) and p_p (θ_p) are the central momenta and angles of the electron spectrometer (C) and the proton spectrometer (B), respectively. Also shown are the four-momentum transfer Q^2 and the p-X relative energy E_{pX}. The average beam current I and the net runtime T are shown in the rightmost columns.

Kinematics	E_0 (MeV)	$\theta_{e'}$	θ_p	$p_{e'}$ (MeV/c)	p_p (MeV/c)	Q^2 (GeV^2/c^2)	E_{pX} (MeV)	I (μA)	T (h)
D-1	659.7	110°	26°	420	444	0.8	0–6	15	181.2
D-2	659.7	110°	26°	420	504	0.8	0–18	15	60.2
D-3	659.7	110°	26°	400	580	0.7	10–45	12.5	68.5
D-4	659.7	110°	26°	385	665	0.7	25–90	15	14.7
D-5	659.7	103°	26°	355	740	0.6	75–145	12.5	29.5
D-6	883.1	107°	25°	485	570	1.2	0–14	10	212.5
D-7	883.1	107°	25°	485	610	1.1	0–24	10	47.0
D-8	883.1	107°	25°	485	713	1.1	10–60	10	3.7
D-9	883.1	92.3°	30°	485	705	0.8	20–80	10	13.5
D-10	883.1	92.3°	30°	485	805	0.8	60–130	10	1.0

elementary pion production process leaving the neutron in the ground state, respectively.

B. The ^{2}H$(e,e'p)X$ reaction

The D$(e,e'p)X$ reaction was studied between May and August 2002 with a total runtime of 632 h. The measured kinematics can be characterized by the relative energy $E_{pX} = W - M_p - M_X$ of the p-X system, where W is the photon-deuteron invariant mass, M_p the proton mass, and M_X the missing mass of the ^{2}H$(e,e'p)X$ reaction. The kinematics of the measured settings varied from the threshold region ($E_{pX} \rightarrow 0$) up to the quasielastic region ($E_{pX} \approx 100$–150 MeV). The near-threshold kinematics have been chosen in analogy to the experiment by Fil'kov *et al.* [3], where the relative energy of the two outgoing nucleons pn (or possibly pX) is small and a strong final-state interaction is expected. In this case, the detected proton is emitted into a small forward cone around the direction of momentum transfer. The kinematical parameters of the measured settings of the ^{2}H$(e,e'p)X$ reaction are listed in Table II.

The ^{2}H$(e,e'p)X$ measurements were carried out simultaneously with a dedicated experiment to measure the electric form factor of the neutron $G_{E,n}$ via the ^{2}H$(\vec{e},e'\vec{n})$ reaction [19]. The $G_{E,n}$ experiment utilized spectrometer A for the scattered electrons and a separate setup to measure the neutron polarization. Spectrometer C (at angles $\gtrsim 90°$ right of the beam) and spectrometer B (at forward angles left of the beam) were used in coincidence for the detection of electrons and protons, respectively, in a parasitic mode. The electron scattering angle was restricted to large values, which, though not optimal, resulted in quite sizable four-momentum transfer Q^2.

The analysis of the missing-mass spectra has been carried out in a way very similar to that of the H$(e,e'\pi^+)X$ measurements described above. To a very large extent, the true $\pi^- p$ coincidence events, which occurred in addition to the random background events, could be identified and removed by requiring a signal in the Čerenkov detector in the electron arm (spectrometer C). Most of the remaining true $\pi^- p$ events could be identified in the coincidence time spectrum, where the $e'p$ and $\pi^- p$ peaks are separated by about 2 ns.

The resulting normalized yields and yield ratios of the ^{2}H$(e,e'p)X$ reaction are presented in Figs. 3 and 4. Figure 3 shows the results of the near-threshold settings, while the results of the quasielastic settings are depicted in Fig. 4. The missing-mass resolution was ≈ 1.3 MeV/c^2 (FWHM) for the near-threshold runs, and ≈ 0.9 (1.3) MeV/c^2 for the runs near the quasielastic maximum. The continuous part of the missing-mass distribution is mainly due to the radiation tail, with the above mentioned $\pi^- p$ background giving a small contribution in the higher missing-mass region. In Fig. 4(b), the pion threshold is open above $M_X > 1070$ MeV/c^2, yielding additional strength. The invariant masses of the states claimed by Tatischeff *et al.* [2] and Fil'kov *et al.* [3] are indicated by the vertical arrows. Here again, as in the case of the hydrogen experiment described above, no significant

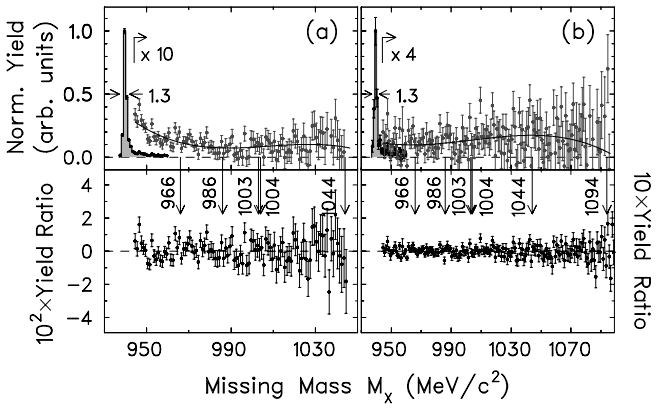

FIG. 3. Upper half: Missing-mass spectra of the ^{2}H$(e,e'p)X$ reaction in the region of the deuteron-breakup threshold at the four-momentum transfer (a) $Q^2 = 0.8$ (GeV/c)^2 and (b) $Q^2 = 1.1$ to 1.2 (GeV/c)^2 (with the neutron peak height set to unity). The plot shows the combined settings (a) D-1,2,3, and (b) D-6,7 (cf. Table II). The achieved missing-mass resolution is ≈ 1.3 MeV/c^2. The solid curves and the yield ratios in the lower half are obtained in the same way as in Fig. 1. Significant structures are excluded to a level of (a) 10^{-2} and (b) 5×10^{-2} of the height of the neutron peak, respectively.

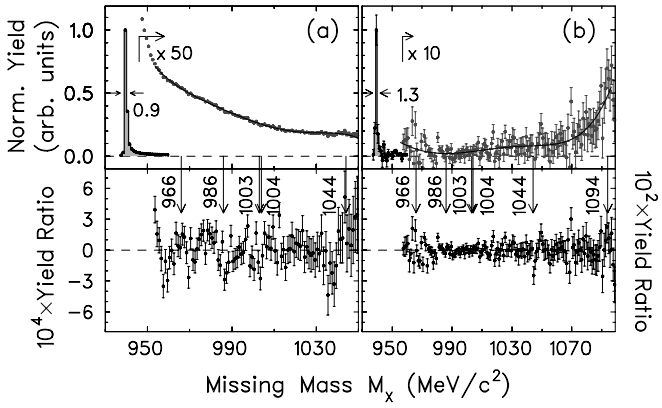

FIG. 4. Upper half: Missing-mass spectra of the ^{2}H$(e,e'p)X$ reaction in the region near the quasielastic peak at (a) $Q^2=0.6$ to 0.7 (GeV/c)^2 and (b) $Q^2=0.8$ to 1.1 (GeV/c)^2 (with the neutron peak height set to unity). The plot shows the combined settings (a) D-4,5 and (b) D-8,9,10 (with the spectrometer settings listed in Table II). The achieved missing-mass resolution is (a) $\approx$0.9 MeV/c^2 and (b) $\approx$1.3 MeV/c^2. The solid curves and the yield ratios in the lower half are obtained in the same way as in Fig. 1. Significant structures are excluded to a level of (a) 10^{-4} and (b) 10^{-2} of the height of the neutron peak, respectively.

peak structure other than the one corresponding to the ground state of the neutron is found. Though the measurements in the threshold region took most of the beamtime (see Table II), the statistics is quite poor even for the ground-state breakup of the deuteron. This is due to the fact that this kinematics maps out very high missing momenta of the proton in the order of 450 MeV/c. In the quasielastic settings (Fig. 4), the cross section is much larger. The differential cross section for the ^{2}H$(e,e'p)$ n channel can be estimated using the deuteron electrodisintegration model of Arenhövel *et al.* [20]. For the threshold settings of Figs. 3(a) and 3(b), one obtains an average of $d^3\sigma/(d\Omega_{e'}dE_{e'}d\Omega_p^*)\approx 1.4\times10^{-6}$ (2.8×10^{-7}) μb/(sr^2 MeV), respectively, whereas the average differential cross section of the quasielastic settings of Fig. 4(a) and 4(b) is about $d^3\sigma/(d\Omega_{e'}dE_{e'}d\Omega_p^*)\approx 1.1\times10^{-3}$ (2.3×10^{-5}) μb/(sr^2 MeV). Significant structures are excluded to a level of 10^{-2} (5×10^{-2}) for the near-threshold settings, and 10^{-4} (10^{-2}) for the quasielastic settings compared to the height of the neutron peak, respectively.

III. SUMMARY

We have searched for narrow structures in the missing-mass spectra of the electromagnetic H$(e,e'\pi^+)X$ and ^{2}H$(e,e'p)X$ reactions in kinematics corresponding to the hadronic beam experiments of Tatischeff *et al.* [2] and Fil'kov *et al.* [3]. Our measurements exclude narrow nucleon resonances below pion threshold for the H$(e,e'\pi^+)X$ reaction down to the level of 10^{-4} compared to the respective transition to the neutron ground state. For the ^{2}H$(e,e'p)X$ reaction, narrow structures are excluded to a level of 10^{-4} relative to the neutron peak in the quasielastic and to 10^{-2} in the near-threshold measurements. On the basis of those results the various theoretical attempts [6,9,10] for an explanation of the observed structures in Refs. [2,3] might be questioned. In order to draw a final conclusion on the existence of the narrow resonances of Refs. [2,3], the hadronic experiments should be repeated with the same accuracy as the present electromagnetic ones.

ACKNOWLEDGMENTS

This work was supported by the Deutsche Forschungsgemeinschaft (Grant Nos. SFB 443 and RI 242/15-2).

[1] A. Thomas and W. Weise, *The Structure of the Nucleon* (Wiley-VCH, Berlin, 2001).
[2] B. Tatischeff, J. Yonnet, N. Willis, M. Boivin, M.P. Comets, P. Courtat, R. Gacougnolle, Y. Le Bornec, E. Loireleux, and F. Reide, Phys. Rev. Lett. **79**, 601 (1997).
[3] L.V. Fil'kov, V.L. Kashevarov, E.S. Konobeevski, M.V. Mordovskoy, S.I. Potashev, V.A. Simonov, V.M. Skorkin, and S.V. Zuev, Eur. Phys. J. A **12**, 369 (2001).
[4] B. Tatischeff, J. Yonnet, M. Boivin, M.P. Comets, P. Courtat, R. Gacougnolle, Y. Le Bornec, E. Loireleux, F. Reide, and N. Willis, Eur. Phys. J. A **17**, 245 (2003); B. Tatischeff, nucl-ex/0207004.
[5] P.J. Mulders, A.T. Aerts, and J.J. de Swart, Phys. Rev. D **21**, 2653 (1980); **19**, 2635 (1979); Phys. Rev. Lett. **40**, 1543 (1978).
[6] N. Konno, Nuovo Cimento Soc. Ital. Fis., A **111A**, 1393 (1998).
[7] A.I. L'vov and R.L. Workman, Phys. Rev. Lett. **81**, 1346 (1998).
[8] V. Olmos de Leon, F. Wissmann, P. Achenbach, J. Ahrens, H.J. Arends, R. Beck, P.D. Harty, V. Hejny, P. Jennewein, M. Kotulla, B. Krusche, V. Kuhr, R. Leukel, J.C. McGeorge, V. Metag, R. Novotny, A. Polonski, F. Rambo, A. Schmidt, M. Schumacher, U. Siodlaczek, H. Ströher, A. Thomas, J. Weiß, and M. Wolf, Eur. Phys. J. A **10**, 207 (2001), and references therein.
[9] A.P. Kobushkin, nucl-th/9804069.
[10] Th. Walcher, hep-ph/0111279.
[11] E.E. Kolomeitsev and D.N. Voskresensky, nucl-th/0207091.
[12] X. Jiang, R. Gilman, R. Ransome, P. Markowitz, T.-H. Chang, C.-C. Chang, G.A. Peterson, D.W. Higinbotham, M.K. Jones, N. Liyanage, and J. Mitchell, Phys. Rev. C **67**, 028201 (2003).
[13] A. Tamii, K. Hatanaka, M. Hatano, D. Hirooka, J. Kamiya, H. Kato, Y. Maeda, T. Saito, H. Sakai, S. Sakoda, K. Sekiguchi, N. Uchigashima, T. Uesaka, T. Wakasa, and K. Yako, Phys. Rev. C **65**, 047001 (2002).
[14] L.V. Fil'kov, nucl-th/0208028.
[15] R. Beck, S.N. Cherepnya, L.V. Fil'kov, V.L. Kashevarov, M. Rost, and Th. Walcher, in *NSTAR Workshop Proceedings*, edited by L. Tiator and D. Drechsel (World Scientific, Singapore, 2001).
[16] K.I. Blomqvist, W.U. Boeglin, R. Böhm, M. Distler, R. Edelhoff, J. Friedrich, R. Geiges, P. Jennewein, M. Kahrau, M.

Korn, H. Kramer, K.W. Krygier, V. Kunde, A. Liesenfeld, H. Merkel, K. Merle, U. Müller, R. Neuhausen, E.A.J.M. Offermann, Th. Pospischil, A.W. Richter, G. Rosner, P. Sauer, St. Schardt, H. Schmieden, A. Wagner, Th. Walcher, and St. Wolf, Nucl. Instrum. Methods Phys. Res. A **403**, 263 (1998).

[17] MAMI-Proposal A1/2-98, 1998.

[18] D. Drechsel, O. Hanstein, S.S. Kamalov, and L. Tiator, Nucl. Phys. **A645**, 145 (1999).

[19] M. Seimetz, in *Baryons 2002*, 9th International Conference on the Structure of Baryons, edited by C.E. Carlson and B.A. Mecking (World Scientific, Singapore, in press).

[20] H. Arenhövel, W. Leidemann, and E.L. Tomusiak, Phys. Rev. C **46**, 455 (1992).